SCHOLARONE™
Manuscripts

Author Manuscript

This is the author manuscript accepted for publication and has undergone full peer review but has not been through the copyediting, typesetting, pagination and proofreading process, which may lead to differences between this version and the Version of record. Please cite this article as doi:10.1002/jum.14616.

1

Fetal Intelligent Navigation Echocardiography (FINE)
Detects 98% of Congenital Heart Disease

Short Running Title: FINE Detection of Congenital Heart Disease

Lami Yeo, MD[1,2,3], Suchaya Luewan, MD[1,4], Roberto Romero, MD, D.Med.Sci.[1,5,6,7]

[1]Perinatology Research Branch, Program for Perinatal Research and Obstetrics, Division of Intramural Research, *Eunice Kennedy Shriver* National Institute of Child Health and Human Development, NIH, Bethesda, MD and Detroit, MI, USA
[2]Detroit Medical Center, Hutzel Women's Hospital, Detroit, MI, USA
[3]Department of Obstetrics and Gynecology, Wayne State University School of Medicine, Detroit, MI, USA
[4]Department of Obstetrics and Gynecology, Chiang Mai University, Chiang Mai, Thailand
[5]Department of Obstetrics and Gynecology, University of Michigan, Ann Arbor, MI, USA
[6]Department of Epidemiology and Biostatistics, Michigan State University, East Lansing, MI, USA
[7]Center for Molecular Medicine and Genetics, Wayne State University, Detroit, MI, USA

Address correspondence to:

Lami Yeo, MD and Roberto Romero, MD, D. Med. Sci.
Perinatology Research Branch, NICHD, NIH, DHHS
Hutzel Women's Hospital
3990 John R, 4 Brush
Detroit, MI 48201, USA
Telephone (313) 993-2700
Fax: (313) 993-2694
E-mail Address: lyeo@med.wayne.edu and prbchiefstaff@med.wayne.edu

Manuscript Category: Original Research

ABSTRACT

Objective: Fetal Intelligent Navigation Echocardiography (FINE) is a novel method that automatically generates and displays nine standard fetal echocardiography views in normal hearts by applying intelligent navigation technology to spatiotemporal image correlation (STIC) volume datasets. The main objective was to determine the sensitivity and specificity of FINE in the prenatal detection of congenital heart disease (CHD).

Methods: A case-control study was conducted in 50 fetuses with a broad spectrum of CHD (cases) and 100 fetuses with normal hearts (controls) in the second and third trimesters. Using four-dimensional ultrasound with STIC technology, volume datasets were acquired. After all identifying information was removed, the datasets were randomly distributed to a different investigator for analysis using FINE. The sensitivity and specificity for the prenatal detection of CHD, as well as positive and negative likelihood ratios (LR) were determined.

Results: The diagnostic performance of FINE for the prenatal detection of CHD was: sensitivity 98% (49/50), specificity 93% (93/100), positive LR of 14, and negative LR of 0.02. Among cases with confirmed CHD, the diagnosis based upon FINE completely matched the final diagnosis in 74% (37/50), minor discrepancies were seen in 12% (6/50), and major discrepancies were seen in 14% (7/50).

Conclusions: We present for the first time the sensitivity and specificity of the FINE method in fetuses with normal hearts and CHD in the second and third trimesters. Since FINE identifies a broad spectrum of CHD with 98% sensitivity, this method could be used prenatally to screen for and diagnose CHD.

3

4

INTRODUCTION

Congenital heart defects (CHD) are the most common birth defect,[1] as well as the leading cause of infant morbidity and mortality from congenital malformations.[2] Screening of all pregnancies is required to detect CHD prenatally, since up to 90% of cases occur in pregnancies without high risk features.[3] Yet, the prenatal detection of CHD has remained challenging, with the sensitivity of ultrasound ranging from 15-39%.[4-12] This has been attributed mainly to operator skill and expertise;[13-18] however, other factors include the complex anatomy, motion, and small size of the fetal heart. The lack of prenatal identification of CHD is associated with adverse consequences for the neonate, including abnormal neurological development, and even death.[19-22] In contrast, the prenatal diagnosis of specific cardiac anomalies improves the preoperative condition,[23-27] pre-surgical mortality rate,[28-30] survival after surgery,[19,23,31,32] and long-term neurocognitive function and outcome.[33,34]

Four-dimensional (4D) ultrasound with spatiotemporal image correlation (STIC) facilitates fetal cardiac examination[35-66] and has the potential to increase the detection rate of CHD,[35,67,68] leading some to propose its clinical application in both prenatal cardiac screening and diagnosis of CHD.[69-75] STIC technology allows the acquisition of a volume dataset of the fetal heart, in which cardiac planes may be extracted and displayed in any orientation.[43,55] However, the use of software to perform manual navigation[76] through such volume datasets is time consuming, highly operator dependent, and requires a thorough knowledge of cardiac anatomy.[77-79] As a result, this process is difficult and impractical, especially when the fetal heart is abnormal.[80]

5

Fetal intelligent navigation echocardiography (FINE) is a novel method developed recently that automatically generates and displays nine standard fetal echocardiography views in normal hearts by applying 'intelligent navigation' technology to STIC volume datasets.[66,76-80] Therefore, such method can simplify examination of the fetal heart and reduce operator dependency. Indeed, studies have reported that FINE applied to STIC volume datasets can successfully generate nine fetal echocardiography views in 96-100%[79] and 98-100%[77,78] of normal hearts in the second and third trimesters. As a result, FINE has been suggested as a method to screen for CHD.[78,79] However, to be clinically useful, a screening test should demonstrate both good specificity and sensitivity.[81] Therefore, we conducted this study to determine the sensitivity and specificity of FINE in the prenatal detection of CHD.

MATERIALS AND METHODS

Subjects

A case-control study of 150 pregnant women having a singleton fetus with a normal heart (100 controls) or confirmed CHD (50 cases) in the second or third trimester was conducted. Patients were examined at the Detroit Medical Center/Wayne State University and the Perinatology Research Branch of NICHD, NIH, DHHS. All women had been enrolled in research protocols approved by the Institutional Review Board of NICHD, NIH, and by the Human Investigation Committee of Wayne State University. All participants provided written informed consent for the use of sonographic images for research purposes. The final diagnosis of CHD was confirmed by neonatal echocardiography and/or other ancillary diagnostic procedures (e.g. surgery, cardiac

6

catheterization, autopsy). In cases when such information was not available, the final diagnosis of CHD was based upon the results of fetal echocardiography performed by an expert.

Spatiotemporal image correlation (STIC) volume datasets

Using STIC technology, sonographic volume datasets of the fetal heart containing gray-scale information were acquired from a four-chamber view by transverse sweeps through the fetal chest in patients examined at our unit. The acquisition time ranged from 10 to 12.5 seconds, depending on fetal motion, and the acquisition angle ranged between 20 and 40 degrees, depending on gestational age.

Volume datasets were selected for analysis using FINE if they met the following criteria: 1) fetal spine located between the 4- and 8-o'clock positions (reducing the possibility of shadowing from the ribs or spine); 2) upper fetal mediastinum and stomach included and visible in the STIC volume; 3) adequate image quality such that fetal anatomy could be visualized; and 4) absence of excessive motion artifacts that could distort anatomic structures. Only a single STIC volume per patient was analyzed.

The following seven major types of CHD were the focus of this study: 1) complete transposition of the great vessels; 2) tetralogy of Fallot; 3) coarctation of the aorta; 4) pulmonary atresia with intact ventricular septum; 5) double outlet right ventricle; 6) hypoplastic left heart; and 7) atrioventricular canal defect. This is justified because such CHD are difficult to diagnose, prenatal diagnosis improves outcome, and some represent a neonatal emergency. However, a broad spectrum of CHD types overall was included to evaluate the diagnostic performance of FINE.

7

Training on the FINE method

One of the investigators (SL) who had no prior familiarity with the FINE method underwent formal training by the same investigators who invented FINE. Such training occurred in a 2-day period and included: 1) attending didactic lectures on FINE; and 2) review of 16 previously acquired STIC volume datasets of normal fetal hearts using the FINE method. Specifically, the following features of FINE were reviewed during the training period (Table 1):[55,76,77,79] 1) intelligent navigation technology; 2) STICLoop™ and STICLoop criteria; 3) Anatomic Box® (learning how to identify and mark anatomical structures of the fetal heart); 4) diagnostic planes; 5) automatic labeling and its features; 6) Virtual Intelligent Sonographer Assistance (VIS-Assistance®) and its advantages in providing additional information, as well as how to perform double and triple VIS-Assistance;[80] and 7) intelligent and marking alerts. Moreover, the same investigator was provided a written manual on FINE and underwent a practical session on how to technically use the system (e.g. review of buttons and screens). It is noteworthy that during the training period, no STIC volumes of CHD cases were reviewed using the FINE method.

Evaluation of STIC volume datasets by FINE

After all identifying information was removed from the 150 STIC volume datasets, they were randomly distributed to the trained investigator for analysis using the FINE method. Such investigator did not acquire any of the STIC volumes, and was blinded to the fetal cardiac diagnosis. To perform the analysis, the STIC volumes were imported into a

software system (5D Heart/Fetal Intelligent Navigation Echocardiography; Version 2015.09.30; Samsung Healthcare, Seoul, Korea) that was installed onto a laptop computer.

The investigator employed all of the features of FINE (e.g. automatic labeling) when interrogating each STIC volume dataset to assist in determining whether the fetal heart was normal or abnormal, and to make a specific diagnosis. When using the Anatomic Box tool, if marking any of the anatomical structures of the fetal heart seemed difficult, the structure was absent (e.g. crux of the heart), or the structure was not in its usual location, the investigator utilized best judgment and estimated the location for marking.

For each STIC volume, VIS-Assistance videoclips were observed in their entirety for all nine fetal echocardiography views since this feature of FINE:[76,77] 1) improves the success of obtaining the fetal echocardiography view of interest; 2) allows operator-independent sonographic navigation and exploration of surrounding structures in the diagnostic plane (i.e. a 'virtual' sonographer); and 3) can show the appropriate azimuth. Written callouts (e.g. "move cephalad") appear at the top of each VIS-Assistance videoclip to inform the operator of the purpose or action of the navigational movements which are occurring automatically. This brings organization to the videoclip and allows operators to use the callouts to target their navigation.

In four cardiac VIS-Assistance views (three vessels and trachea, left ventricular outflow tract, short-axis view of great vessels/right ventricular outflow tract and abdomen/stomach) for normal hearts, we pre-specified that certain anatomical structures should also be visualized in order to consider the VIS-Assistance as being successful in depicting the echocardiography view; this has been reported elsewhere.[77,78]

9

Using the FINE method, the investigator initially determined whether the fetal heart was normal or abnormal, and then recorded the following information, respectively:

- Normal heart: 1) fulfillment of all nine STICLoop criteria; 2) appearance of intelligent and/or marking alerts; 3) success rate of generating each of the nine echocardiography views using diagnostic planes and/or VIS-Assistance.

- Abnormal heart (CHD): 1) fulfillment of all nine STICLoop criteria; 2) appearance of intelligent and/or marking alerts; 3) frequency of abnormal echocardiography views (out of nine); 4) which echocardiography views were abnormal and a description of the findings (e.g. ventricular septal defect); 5) whether diagnostic planes and/or VIS-Assistance views were abnormal; 6) use of the double or triple VIS-Assistance technique; 7) correct or incorrect labeling of anatomical structures; 8) summary of individual findings (e.g. overriding aorta) and the final presumptive diagnosis (e.g. tetralogy of Fallot).

The sensitivity and specificity of FINE for the prenatal detection of CHD, as well as positive and negative likelihood ratios were determined. Finally, among cases with confirmed CHD, the degree of concordance with the diagnosis based upon the FINE method was categorized as follows: 1) category A: complete agreement; 2) category B: minor discrepancies in the diagnosis; and 3) category C: major discrepancies in the diagnosis.

RESULTS

A total of 150 STIC volume datasets (100 controls and 50 cases) were evaluated using the FINE method. The median gestational age at the time of STIC volume

acquisition was 25 (interquartile range, 22 – 29) weeks. However, STIC volumes were obtained from 16 to 37 weeks of gestation, with 36% (54/150) of fetuses being in the third trimester.

Normal Fetal Hearts Evaluated by FINE

STICLoop criteria

All 100 STIC volumes of normal hearts were initially evaluated by STICLoop criteria (Table 1). Seven of the nine criteria were met 95-99% of the time. For example, in 99% (99/100) of STIC volumes, the upper mediastinum and stomach were included within the volume and clearly visible. However, approximately 20% of the STIC volumes of normal hearts did not meet the following STICLoop criteria: 1) minimal or absent shadowing (21%; n=21); and 2) minimal or no motion artifacts observed in the STICLoop (23%; n=23). Therefore, the investigator recorded that 23% of such STIC volumes contained motion artifacts.

Intelligent and marking alerts

While marking anatomical structures of the normal fetal heart within the STIC volume (using the feature Anatomic Box), an intelligent alert automatically appeared in 27% (27/100): 1) breech alert in 18% (n=18); 2) possible drifting spine alert in 5% (n=5); and 3) spine location alert in 4% (n=4). Therefore, 18% of the fetuses were in an original breech presentation so that the cardiac apex was originally pointing to the right side of the monitor screen. The spine location alert appeared in only 4% of the volumes, and such alert was automatically activated during the marking process because the fetal spine in the STIC volume was located in a position other than between 5- and 7-o'clock: 1) 7- to 8-

11

o'clock in 75% (n=3) and 2) 8-o'clock in 25% (n=1). Therefore, 96 STIC volumes had a fetal spine located at 5, 6, or 7-o'clock. Each time the spine location alert was activated, three marking alerts (pulmonary valve, superior vena cava, and transverse aortic arch) appeared next in sequence. These marking alerts "informed" the investigator (through captions and a movie) that fetal anatomical structures for marking (e.g. superior vena cava) could be in a different location than expected, since the fetal spine was not located between the 5- and 7-o'clock positions.

Success rates of generating fetal echocardiography views

For the 100 normal hearts, the FINE method was able to successfully generate nine fetal echocardiography views using: 1) diagnostic planes in 94-100% of cases; 2) VIS-Assistance in 100% of cases; and 3) a combination of diagnostic planes and/or VIS-Assistance in 100% of cases (Table 2). Figure 1 and Video 1 show an example of nine normal cardiac diagnostic planes in a single template with the additional feature of automatic labeling through intelligent navigation.

Congenital Heart Disease Cases Evaluated by FINE

Of the 50 cases, the main categories of CHD included (Table 3): 1) conotruncal anomalies (42%; n=21); 2) left heart anomalies (20%; n=10); 3) right heart anomalies (16%; n=8); 4) complex cardiac defects (12%; n=6); and 5) septal defects (10%; n=5).

STICLoop criteria

All STIC volumes of CHD were initially evaluated by STICLoop criteria (Table 1). Two of the nine criteria were met 98% of the time. For example, 98% (98/100) of the STIC volumes included the upper mediastinum and stomach, which were clearly visible.

However, 50% (25/50) of the STIC volumes of CHD contained motion artifacts. Moreover, the investigator recorded that 20% (10/50) and 26% (13/50) of CHD volumes were characterized by inadequate image quality and shadowing, respectively.

Intelligent and marking alerts

For CHD, while marking anatomical structures of the fetal heart within the STIC volume (using the feature Anatomic Box), an intelligent alert automatically appeared in 42% (21/50): 1) spine location alert in 20% (n=10); 2) breech alert in 12% (n=6); and 3) possible drifting spine alert in 10% (n=5). Therefore, 12% of the fetuses were in an original breech presentation so that the cardiac apex was originally pointing to the right side of the monitor screen. The spine location alert was automatically activated during the marking process because the fetal spine in the STIC volume was located in a position other than between 5- and 7-o'clock: 1) 7- to 8-o'clock in 50% (n=5); 2) 4- to 5-o'clock in 30% (n=3); and 3) 4-o'clock in 20% (n=2). For each spine location alert activated, three marking alerts (pulmonary valve, superior vena cava, and transverse aortic arch) appeared next in sequence.

Abnormal fetal echocardiography views generated by FINE

Eighty percent (40/50) of the STIC volumes of CHD had six to nine abnormal fetal echocardiography views (diagnostic planes and/or VIS-Assistance) (Figure 2 and Figure 3; Video 2 and Video 3): 1) nine abnormal views (8%; n=4); 2) eight abnormal views (42%; n=21); 3) seven abnormal views (16%; n=8); and 4) six abnormal views (14%; n=7). Therefore, of all the CHD cases, approximately half of them had eight abnormal fetal

echocardiography views generated by FINE, making it highly likely that an operator would recognize the heart to be abnormal.

Of all the cases, 96% (48/50) and 94% (47/50) had an abnormal five-chamber view and left ventricular outflow tract view via FINE, respectively, making these the most frequent abnormal fetal echocardiography views in our study. In contrast, only 10% (5/50) of CHD cases had an abnormal vena cava view.

VIS-Assistance and automatic labeling

When implementing VIS-Assistance for the CHD cases, the following advantages were noted (Table 4): 1) depicted cardiac abnormalities when the diagnostic plane appeared normal; 2) provided further diagnostic information even when the diagnostic plane was abnormal (Figure 4 and Video 4); 3) changed a suspected abnormal fetal echocardiography view to one that was interpreted as normal; and 4) improved the success of obtaining the fetal echocardiography view of interest when this was not initially obtained via the diagnostic plane.

To gain further assistance in determining the CHD diagnosis and obtaining more information, the investigator employed *double VIS-Assistance* (Table 1) in 56% (28/50) of the STIC volumes for one to three fetal echocardiography views. On the other hand, *triple VIS-Assistance* (Table 1) was activated for only 10% (5/50) of the STIC volumes for one to two fetal echocardiography views.

It is noteworthy that even though the fetal cardiac anatomy was abnormal for all 50 cases, the FINE method was able to automatically generate the correct labeling of

anatomical structures (atrial and ventricular chambers, great vessels, venae cavae, and stomach) for all nine fetal echocardiography views in 74% (37/50) of cases.

Diagnostic Performance of FINE

The overall sensitivity, specificity, positive and negative likelihood ratios of FINE for the prenatal detection of CHD was 98% (49/50), 93% (93/100), 14, and 0.02, respectively. The seven false-positive diagnoses included: 1) six fetuses suspected to have ventricular septal defects (gestational ages ranged from 19 to 31 weeks); and 2) one fetus with a suspected cardiac tumor in the right ventricle (29 weeks of gestation). The single false-negative case was a fetus examined by FINE at 26 weeks of gestation who was later diagnosed with pulmonary artery branch stenosis and a small secundum atrial septal defect in the neonatal period.

Complete concordance (category A) or a minor discrepancy (category B) between the diagnosis based on FINE and the final CHD diagnosis occurred in 86% (43/50) of cases: 1) complete concordance (54%; n=27); and 2) minor discrepancy (32%; n=16). All of the discordant diagnoses in category B were related to: 1) secundum atrial septal defect (75%; n=12); 2) ventricular septal defect (19%; n=3); 3) left superior vena cava (19%; n=3); and 4) primum atrial septal defect (6%; n=1). Major differences (category C) between the FINE and final CHD diagnoses occurred in only 14% (n=7) of cases (Table 5).

It is noteworthy that when we excluded from category B cases in which the only discrepancy between the FINE diagnosis and the final CHD diagnosis was a secundum atrial septal defect, then 10 cases would be re-classified into category A with the following

new classification results: 1) complete concordance (74%; n=37); 2) minor discrepancy (12%; n=6); and 3) major discrepancy (14%; n=7). Such re-classification is justified because the diagnosis of a secundum atrial septal defect is almost nonexistent in the prenatal period.[82]

DISCUSSION

Principal findings of the study

After applying the FINE method to STIC volume datasets acquired with gray-scale information in second and third trimester fetuses with normal and abnormal hearts: 1) the sensitivity, specificity, positive and negative likelihood ratios of FINE for the prenatal detection of CHD was 98%, 93%, 14, and 0.02 respectively; 2) among cases with confirmed CHD, the diagnosis based upon FINE completely matched the final diagnosis in 74%, minor discrepancies were seen in 12%, and major discrepancies were seen in 14%; 3) 80% of the CHD cases had six to nine abnormal fetal echocardiography views out of nine, making it highly likely that the heart would be recognized as abnormal; 4) automatic labeling of anatomical structures in all nine fetal echocardiography views was correct in 74% of CHD cases; and 5) nine fetal echocardiography views were generated successfully in normal hearts using diagnostic planes in 94-100% of cases, VIS-Assistance in 100% of cases, and a combination of diagnostic planes and/or VIS-Assistance in 100% of cases.

Performance of 4D sonography with STIC in the prenatal detection of CHD

At the time of its original conception and development, we proposed using the FINE method as an aid to examine the fetal heart in the population at large, rather than to diagnose specific CHD.[77] Indeed, we had speculated that for some types of CHD, the FINE

method may not be useful or applicable (e.g. hypoplastic left heart, atrioventricular canal defect).[77] However, since that time we have gained considerable experience in the application of FINE and color Doppler FINE to a broad spectrum of CHD types,[66,77,80] and concluded that such technology is both successful and informative. For example, in a case of fetal dextrocardia and situs solitus with complex CHD, FINE was invaluable in diagnosing multiple abnormalities and defining complex anatomic relationships, which had been very difficult to do using real-time echocardiography.[80]

However, for a test to be clinically useful it should demonstrate both high specificity and sensitivity. As a result, we set out to determine the diagnostic performance of FINE, and report for the first time herein that there is 98% sensitivity and 93% specificity for the prenatal detection of a broad spectrum of CHD. This outcome was obtained despite the fact that approximately 20% of STIC volumes of normal hearts had shadowing present, or contained motion artifacts. Moreover, STIC volumes of CHD were characterized by inadequate image quality, shadowing, or motion artifacts in 20%, 26%, and 50% of cases, respectively. Therefore, not all the volumes analyzed in this study were ideal or optimal. Recently, an electronic matrix 4D probe has been developed which allows a marked reduction in the STIC volume acquisition time (which could lead to less motion artifacts), as well as improved image resolution in the B plane.[55,83] Such electronic STIC volumes have been shown to be of more significant optimal diagnostic quality compared to conventional STIC volumes.[84] Therefore, this new STIC technology could be advantageous for the FINE method.

Likelihood ratios summarize how many times more (or less) likely patients with the disease are to have that particular result than patients without the disease.[85] The further likelihood ratios are from 1, the stronger the evidence for the presence or absence of disease. Indeed, likelihood ratios >10 and < 0.1 are considered to provide strong evidence to rule in or rule out diagnoses, respectively, in most circumstances.[85,86] Thus, in the current study, the positive (14) and negative likelihood ratios (0.02) indicate that results of the FINE method have a large effect on increasing or decreasing, respectively, the probability of the presence of CHD.

Prior investigators have examined the diagnostic performance of 4D sonography with STIC by using a display modality[87] or manual navigation (retrieval and display of relevant cardiac diagnostic planes by interrogating volume datasets).[70,72-74] Bennasar et al. used the multiplanar view to analyze STIC volumes of normal and abnormal fetal hearts, and reported an overall sensitivity and specificity of 94.9% (166/175) and 88.1% (141/160), respectively.[72] STIC volumes had been acquired with both gray-scale and color Doppler information. In a multi-center study of seven centers with expertise in 4D ultrasound of the fetal heart, 90 STIC volume datasets of normal (n=45) or abnormal fetal hearts (n=45) acquired at 18-26 gestational weeks using B-mode or color Doppler sonography were blindly evaluated by all centers.[73] The approach used to analyze the volumes was left to the discretion of each center. Overall, the median (range) sensitivity and specificity for the identification of fetuses with CHD were 93% (77-100%) and 96% (84-100%).[73] Years ago, our team used tomographic ultrasound imaging (TUI) in combination with B-mode STIC volume datasets to diagnose CHD, and reported a

sensitivity and specificity of 85.7% (12/14) and 100% (101/101), respectively.[87] However, such study performance was based on only 14 cases with CHD. Paladini et al. investigated whether fourteen sonologists could detect major abnormalities of the outflow tracts by reviewing the A plane of 16 normal and 10 abnormal STIC volume datasets.[70] The sensitivity and specificity were reported as 83% and 87%, respectively. The individual diagnostic accuracy ranged from 66-100% (median 85.5%).[70] In contrast, Adriaanse et al. evaluated the clinical accuracy of 4D ultrasound with STIC in a telemedicine setting.[74] Ten STIC volumes from the second trimester were analyzed by 3 different observers using any desired post-processing modality (e.g. sectional planes, rendering, TUI). The authors concluded that while STIC by telemedicine is promising, it was not accurate enough for exclusive use in clinical decision making regarding treatment, prognosis, etc.[74]

Taken together, while most of these studies reported high sensitivity and specificity in the detection of CHD, STIC volume analysis required manual standardization or manipulation of the dataset and reference planes by the operator, or was dependent on the TUI display. Yet, operator dependency is reported to be the main problem when STIC volumes are analyzed.[67] On the other hand, the FINE method substantially decreases the number of steps required to obtain echocardiography views, making this method less operator dependent and considerably simplifying the fetal cardiac examination.[77] The sonologist is only required to mark anatomical structures of the fetal heart within the STIC volume dataset, triggering intelligent navigation technology and resulting in the successful generation of nine echocardiography views automatically (this occurred in 100% of normal hearts via a combination of diagnostic planes and/or VIS-Assistance for the study herein).

19

For CHD cases analyzed using FINE, abnormal cardiac anatomy was evident in multiple echocardiography views simultaneously. A summary of the characteristics of the FINE method that are fundamental in determining whether the fetal heart is abnormal or not, and in determining the type of CHD are described in Table 4.

Comparisons between FINE and final diagnoses

There were seven false-positive diagnoses of ventricular septal defects based upon FINE, which would not have had a major impact on clinical outcome. Similarly, Bennasar et al. reported that 52% (10/19) of their false-positive diagnoses from STIC echocardiography were ventricular septal defects.[72] The accurate prenatal detection of ventricular septal defects can be influenced by both the location and size of the defect, as well as drop-out artifacts. It is possible that if STIC volumes had been obtained with color or power Doppler information and analyzed by FINE (i.e. color Doppler FINE)[66] in the current study, the number of false-positive diagnoses would have been reduced.

Among cases with confirmed CHD, the diagnosis based upon FINE completely matched the final diagnosis in 74%, minor discrepancies were seen in 12%, and major discrepancies were seen in 14%. Such results are very similar to a different study in which the authors examined the concordance of prenatal and postnatal echocardiograms performed by specialized pediatric cardiologists in a large referral center.[88] Overall, the prenatal diagnosis precisely matched the postnatal diagnosis in 69.8%, minor discrepancies were seen in 14.2%, and major differences were seen in 16% of cases. Similarly, among cases with confirmed CHD, Bennasar reported that using STIC echocardiography, there was absolute concordance with the final diagnosis in 74.3%.[72]

Of the 7 cases with major differences between the FINE diagnosis and final CHD diagnosis (category C), 43% (n=3) were conotruncal abnormalities (Table 5). Prior studies have shown that conotruncal anomalies are the CHD in which discrepancies with the postnatal diagnosis are the most common.[89-92]

Clinical implications of the study

Based upon the study herein, there are several clinical implications regarding the FINE method: 1) it may be used to assess fetuses with normal hearts and a broad spectrum of CHD with a high sensitivity and specificity; 2) it can be considered both a cardiac screening and diagnostic tool in the clinical setting; 3) since STIC volume datasets, diagnostic planes, and VIS-Assistance videoclips can be transmitted by telemedicine for expert consultation, this expands the outreach of fetal cardiac imaging, which could favorably impact the current sensitivity of CHD; and 4) it can be used for educational and training purposes.

Limitations

In cases of CHD, only a single STIC volume per fetus was examined using FINE. It is possible that by examining multiple STIC volume datasets at a given gestational age, or examining STIC volumes over time, this would have led to improved and/or different diagnostic information (e.g. some CHD are progressive). The FINE method is not meant to replace real-time fetal echocardiography, since the latter allows evaluation of cardiac rate or rhythm disturbances, the performance of pulsed wave Doppler velocimetry, etc. Therefore, when fetal CHD is suspected, such patients should then undergo real-time sonographic examination by an appropriate sonologist (e.g. pediatric cardiologist). Finally,

21

studies are required to determine the learning curve for FINE among operators with varying levels of experience.

Conclusions

We present herein for the first time the sensitivity and specificity of the FINE method in fetuses with normal hearts and CHD in the second to third trimesters. Since FINE identifies a broad spectrum of CHD with 98% sensitivity, this method could be used prenatally to screen for and diagnose CHD.

ACKNOWLEDGMENTS

23

REFERENCES

1. Simeone RM, Feldkamp ML, Reefhuis J, et al. CDC Grand Rounds: Understanding the Causes of Major Birth Defects - Steps to Prevention. *MMWR Morb Mortal Wkly Rep* 2015; 64:1104-1107.

2. Yang Q, Chen H, Correa A, Devine O, Mathews TJ, Honein MA. Racial differences in infant mortality attributable to birth defects in the United States, 1989-2002. *Birth Defects Res A Clin Mol Teratol* 2006; 76:706-713.

3. Allan L. Antenatal diagnosis of heart disease. *Heart* 2000; 83:367.

4. Friedberg MK, Silverman NH, Moon-Grady AJ, et al. Prenatal detection of congenital heart disease. *J Pediatr* 2009; 155:26-31.

5. Jaeggi ET, Sholler GF, Jones OD, Cooper SG. Comparative analysis of pattern, management and outcome of pre- versus postnatally diagnosed major congenital heart disease: a population-based study. *Ultrasound Obstet Gynecol* 2001; 17:380-385.

6. Acherman RJ, Evans WN, Luna CF, et al. Prenatal detection of congenital heart disease in southern Nevada: the need for universal fetal cardiac evaluation. *J Ultrasound Med* 2007; 26:1715-1719.

7. Garne E, Stoll C, Clementi M. Evaluation of prenatal diagnosis of congenital heart diseases by ultrasound: experience from 20 European registries. *Ultrasound Obstet Gynecol* 2001; 17:386-391.

8. Westin M, Saltvedt S, Bergman G, et al. Routine ultrasound examination at 12 or 18 gestational weeks for prenatal detection of major congenital heart

malformations? A randomized controlled trial comprising 36,299 fetuses. *BJOG* 2006; 113:675-682.

9. Nikkila A, Bjorkhem G, Kallen B. Prenatal diagnosis of congenital heart defects – a population based study. *Acta Paediatr* 2007; 96:49-52.

10. Pinto NM, Keenan HT, Minich LL, Puchalski MD, Heywood M, Botto LD. Barriers to prenatal detection of congenital heart disease: a population based study. *Ultrasound Obstet Gynecol* 2012; 40:418-425.

11. McBrien A, Sands A, Craig B, Dornan J, Casey F. Major congenital heart disease: antenatal detection, patient characteristics and outcomes. J *Matern Fetal Neonatal Med* 2009; 22:101-105.

12. Sklansky MS, Berman DP, Pruetz JD, Chang RK. Prenatal screening for major congenital heart disease: superiority of outflow tracts over the 4-chamber view. *J Ultrasound Med* 2009; 28:889-899.

13. Allan L, Benacerraf B, Copel JA, et al. Isolated major congenital heart disease. *Ultrasound Obstet Gynecol* 2001; 17:370-379.

14. Carvalho JS, Mavrides E, Shinebourne EA, Campbell S, Thilaganathan B. Improving the effectiveness of routine prenatal screening for major congenital heart defects. *Heart* 2002; 88:387-391.

15. Hunter S, Heads A, Wyllie J, Robson S. Prenatal diagnosis of congenital heart disease in the northern region of England: benefits of a training programme for obstetric ultrasonographers. *Heart* 2000; 84:294-298.

25

16. Rustico MA, Benettoni A, D'Ottavio G, et al. Early screening for fetal cardiac anomalies by transvaginal echocardiography in an unselected population: the role of operator experience. *Ultrasound Obstet Gynecol* 2000; 16:614-619.

17. Tegnander E, Eik-Nes SH. The examiner's ultrasound experience has a significant impact on the detection rate of congenital heart defects at the second-trimester fetal examination. *Ultrasound Obstet Gynecol* 2006; 28:8-14.

18. Wong SF, Chan FY, Cincotta RB, Lee-Tannock A, Ward C. Factors influencing the prenatal detection of structural congenital heart diseases. *Ultrasound Obstet Gynecol* 2003; 21:19-25.

19. Franklin O, Burch M, Manning N, Sleeman K, Gould S, Archer N. Prenatal diagnosis of coarctation of the aorta improves survival and reduces morbidity. *Heart* 2002; 87:67-69.

20. Acherman RJ, Evans WN, Luna CF, et al. Prenatal detection of congenital heart disease in southern Nevada: the need for universal fetal cardiac evaluation. *J Ultrasound Med* 2007; 26:1715-1719.

21. Tibballs J, Cantwell-Barti A. Outcomes of management decisions by parents for their infants with hypoplastic left heart syndrome born with and without a prenatal diagnosis. *J Paediatr Child Health* 2008; 44:321-324.

22. Daubeney PE, Sharland GK, Cook AC, Keeton BR, Anderson RH, Webber SA. Pulmonary atresia with intact ventricular septum: impact of fetal echocardiography on incidence at birth and postnatal outcome. UK and Eire Collaborative Study of Pulmonary Atresia with Intact Ventricular Septum. *Circulation* 1998; 98:562-566.

23. Tworetzky W, McElhinney DB, Reddy VM, Brook MM, Hanley FL, Silverman NH. Improved surgical outcome after fetal diagnosis of hypoplastic left heart syndrome. *Circulation* 2001; 103:1269-1273.

24. Kumar RK, Newburger JW, Gauvreau K, Kamenir SA, Hornberger LK. Comparison of outcome when hypoplastic left heart syndrome and transposition of the great arteries are diagnosed prenatally versus when diagnosis of these two conditions is made only postnatally. *Am J Cardiol* 1999; 83:1649-1653.

25. Verheijen PM, Lisowski LA, Stoutenbeek P, Hitchcock JF, Bennink GK, Meijboom EJ. Lactacidosis in the neonate is minimized by prenatal detection of congenital heart disease. *Ultrasound Obstet Gynecol* 2002; 19:552-555.

26. Schultz AH, Localio AR, Clark BJ, Ravishankar C, Videon N, Kimmel SE. Epidemiologic features of the presentation of critical congenital heart disease: implications for screening. *Pediatrics* 2008; 121:751-757.

27. Brown KL, Ridout DA, Hoskote A, Verhulst L, Ricci M, Bull C. Delayed diagnosis of congenital heart disease worsens preoperative condition and outcome of surgery in neonates. *Heart* 2006; 92:1298-1302.

28. van Velzen CL, Haak MC, Reijnders G, et al. Prenatal detection of transposition of the great arteries reduces mortality and morbidity. *Ultrasound Obstet Gynecol* 2015; 45:320-325.

29. Holland BJ, Myers JA, Woods CR Jr. Prenatal diagnosis of critical congenital heart disease reduces risk of death from cardiovascular compromise prior to planned

neonatal cardiac surgery: a meta-analysis. *Ultrasound Obstet Gynecol* 2015; 45:631-638.

30. Grinenco S, Meller C, Marantz P, Izbizky G. Prenatal diagnosis of congenital heart disease: improving survival. *Ultrasound Obstet Gynecol* 2015; 46:633.

31. Bonnet D, Coltri A, Butera G, et al. Detection of transposition of the great arteries in fetuses reduces neonatal morbidity and mortality. *Circulation* 1999; 99:916-918.

32. Khoshnood B, De Vigan C, Vodovar V, et al. Trends in prenatal diagnosis, pregnancy termination, and perinatal mortality of newborns with congenital heart disease in France, 1983-2000: a population-based evaluation. *Pediatrics* 2005; 115:95-101.

33. Kipps AK, Feuille C, Azakie A, et al. Prenatal diagnosis of hypoplastic left heart syndrome in current era. *Am J Cardiol* 2011; 108:421-427.

34. Mahle WT, Clancy RR, McGaurn SP, Goin JE, Clark BJ. Impact of prenatal diagnosis on survival and early neurologic morbidity in neonates with the hypoplastic left heart syndrome. *Pediatrics* 2001; 107:1277-1282.

35. DeVore GR, Falkensammer P, Sklansky MS, Platt LD. Spatiotemporal image correlation (STIC): new technology for evaluation of the fetal heart. *Ultrasound Obstet Gynecol* 2003; 22:380-387.

36. Goncalves LF, Lee W, Chaiworapongsa T, et al. Four-dimensional ultrasonography of the fetal heart with spatiotemporal image correlation. *Am J Obstet Gynecol* 2003; 189:1792-1802.

37.   Chaoui R, Hoffmann J, Heling KS. Three-dimensional (3D) and 4D color Doppler fetal echocardiography using spatio-temporal image correlation (STIC). *Ultrasound Obstet Gynecol* 2004; 23:535-545.

38.   Molina FS, Faro C, Sotiriadis A, Dagklis T, Nicolaides KH. Heart stroke volume and cardiac output by four-dimensional ultrasound in normal fetuses. *Ultrasound Obstet Gynecol* 2008; 32:181-187.

39.   Tutschek B, Sahn DJ. Semi-automatic segmentation of fetal cardiac cavities: progress towards an automated fetal echocardiogram. *Ultrasound Obstet Gynecol* 2008; 32:176-180.

40.   Zhao L, Wu Y, Chen S, et al. Feasibility study on prenatal cardiac screening using four-dimensional ultrasound with spatiotemporal image correlation: a multicenter study. *PLoS One* 2016; 11:e0157477.

41.   Avnet H, Mazaaki E, Shen O, Cohen S, Yagel S. Evaluating spatiotemporal image correlation technology as a tool for training nonexpert sonographers to perform examinations of the fetal heart. *J Ultrasound Med* 2016; 35:111-119.

42.   Bennasar M, Martínez JM, Olivella A, et al. Feasibility and accuracy of fetal echocardiography using four-dimensional spatiotemporal image correlation technology before 16 weeks' gestation. *Ultrasound Obstet Gynecol* 2009; 33:645-651.

43.   Yeo L, Romero R. How to acquire cardiac volumes for sonographic examination of the fetal heart: Part 1. *J Ultrasound Med* 2016; 35: 1021-1042.

44. Novaes JY, Zamith MM, Araujo Junior E, Barreto EQ, Barros FS, Moron AF. Screening of congenital heart diseases by three-dimensional ultrasound using spatiotemporal image correlation: influence of professional experience. *Echocardiography* 2016; 33: 99-104.

45. Jantarasaengaram S, Vairojanavong K: Eleven fetal echocardiographic planes using 4-dimensional ultrasound with spatio-temporal image correlation (STIC): a logical approach to fetal heart volume analysis. *Cardiovasc Ultrasound* 2010; 8:41.

46. Crispi F, Gratacós E. Fetal cardiac function: technical considerations and potential research and clinical applications. *Fetal Diagn Ther* 2012; 32:47-64.

47. Cohen L, Mangers K, Grobman WA, Platt LD. Satisfactory visualization rates of standard cardiac views at 18 to 22 weeks' gestation using spatiotemporal image correlation. *J Ultrasound Med* 2009; 28:1645-1650.

48. Luewan S, Yanase Y, Tongprasert F, Srisupundit K, Tongsong T. Fetal cardiac dimensions at 14-40 weeks' gestation obtained using cardio-STIC-M. *Ultrasound Obstet Gynecol* 2011; 37:416-422.

49. Uittenbogaard LB, Haak MC, Spreeuwenberg MD, van Vugt JM. Fetal cardiac function assessed with four-dimensional ultrasound imaging using spatiotemporal image correlation. *Ultrasound Obstet Gynecol* 2009; 33:272-281.

50. Yeo L, Romero R, Jodicke C, et al. Simple targeted arterial rendering (STAR) technique: a novel and simple method to visualize the fetal cardiac outflow tracts. *Ultrasound Obstet Gynecol* 2011; 37:549-556.

51. Espinoza J, Kusanovic JP, Goncalves LF, et al. A novel algorithm for comprehensive fetal echocardiography using 4-dimensional ultrasonography and tomographic imaging. *J Ultrasound Med* 2006; 25:947-956.

52. Araujo Junior E, Rolo LC, Rocha LA, Nardozza LM, Moron AF. The value of 3D and 4D assessments of the fetal heart. *Int J Womens Health* 2014; 6:501-507.

53. Goncalves LF, Romero R, Espinoza J, et al. Four-dimensional ultrasonography of the fetal heart using color Doppler spatiotemporal image correlation. *J Ultrasound Med* 2004; 23:473-481.

54. Turan S, Turan OM, Ty-Torredes K, Harman CR, Baschat AA. Standardization of the first-trimester fetal cardiac examination using spatiotemporal image correlation with tomographic ultrasound and color Doppler imaging. *Ultrasound Obstet Gynecol* 2009; 33:652-656.

55. Yeo L, Romero R. How to acquire cardiac volumes for sonographic examination of the fetal heart: Part 2. *J Ultrasound Med* 2016; 35:1043-1066.

56. Yagel S, Cohen SM, Shapiro I, Valsky DV. 3D and 4D ultrasound in fetal cardiac scanning: a new look at the fetal heart. *Ultrasound Obstet Gynecol* 2007; 29:81-95.

57. Rizzo G, Capponi A, Muscatello A, Cavicchioni O, Vendola M, Arduini D. Examination of the fetal heart by four-dimensional ultrasound with spatiotemporal image correlation during routine second-trimester examination: the 'three-steps technique'. *Fetal Diagn Ther* 2008; 24:126-131.

58. Hamill N, Yeo L, Romero R, et al. Fetal cardiac ventricular volume, cardiac output, and ejection fraction determined with 4-dimensional ultrasound using spatiotemporal image correlation and virtual organ computer-aided analysis. *Am J Obstet Gynecol* 2011; 205:76.e1-10.

59. Barros FS, Moron AF, Rolo LC, et al. Fetal myocardial wall area: constructing a reference range by means of spatiotemporal image correlation in the rendering mode. *Fetal Diagn Ther* 2015; 37:44-50.

60. DeVore GR, Polanco B, Sklansky MS, Platt LD. The 'spin' technique: a new method for examination of the fetal outflow tracts using three-dimensional ultrasound. *Ultrasound Obstet Gynecol* 2004; 24:72-82.

61. Yeo L, Romero R, Jodicke C, et al. Four-chamber view and 'swing technique' (FAST) echo: a novel and simple algorithm to visualize standard fetal echocardiographic planes. *Ultrasound Obstet Gynecol* 2011; 37:423-431.

62. Nardozza LM, Rolo LC, Araujo Júnior E, et al. Reference range for fetal interventricular septum area by means of four-dimensional ultrasonography using spatiotemporal image correlation. *Fetal Diagn Ther* 2013; 33:110-115.

63. Viñals F. Current experience and prospect of internet consultation in fetal cardiac ultrasound. *Fetal Diagn Ther* 2011; 30:83-87.

64. Godfrey ME, Messing B, Valsky DV, Cohen SM, Yagel S. Fetal cardiac function: M-mode and 4D spatiotemporal image correlation. *Fetal Diagn Ther* 2012; 32:17-21.

65. Abuhamad A, Chaoui R. Three-dimensional fetal echocardiography: basic and advanced applications. In: Abuhamad A, Chaoui R (eds). *A Practical Guide to Fetal Echocardiography: Normal and Abnormal Hearts*. Philadelphia, PA: Lippincott Williams & Wilkins; 2010: 110-127.

66. Yeo L, Romero R. Color and power Doppler combined with fetal intelligent navigation echocardiography (FINE) to evaluate the fetal heart. *Ultrasound Obstet Gynecol* 2017; 50:476-491.

67. Adriaanse BM, van Vugt JM, Haak MC. Three- and four-dimensional ultrasound in fetal echocardiography: an up-to-date overview. *J Perinatol* 2016; 36: 685-693.

68. Espinoza J. Contemporary clinical applications of spatio-temporal image correlation in prenatal diagnosis. *Curr Opin Obstet Gynecol* 2011; 23:94-102.

69. Goncalves LF, Espinoza J, Romero R, et al. A systematic approach to prenatal diagnosis of transposition of the great arteries using 4-dimensional ultrasonography with spatiotemporal image correlation. *J Ultrasound Med* 2004; 23:1225-1231.

70. Paladini D, Sglavo G, Greco E, Nappi C. Cardiac screening by STIC: can sonologists performing the 20-week anomaly scan pick up outflow tract abnormalities by scrolling the A-plane of STIC volumes? *Ultrasound Obstet Gynecol* 2008; 32:865-870.

71. Gindes L, Hegesh J, Weisz B, Gilboa Y, Achiron R. Three and four dimensional ultrasound: a novel method for evaluating fetal cardiac anomalies. *Prenat Diagn* 2009; 29:645-653.

33

72.   Bennasar M, Martínez JM, Gómez O, et al. Accuracy of four-dimensional spatiotemporal image correlation echocardiography in the prenatal diagnosis of congenital heart defects. *Ultrasound Obstet Gynecol* 2010; 36:458-464.

73.   Espinoza J, Lee W, Comstock C, et al. Collaborative study on 4-dimensional echocardiography for the diagnosis of fetal heart defects: the COFEHD study. *J Ultrasound Med* 2010; 29:1573-1580.

74.   Adriaanse BM, Tromp CH, Simpson JM, et al. Interobserver agreement in detailed prenatal diagnosis of congenital heart disease by telemedicine using four-dimensional ultrasound with spatiotemporal image correlation. *Ultrasound Obstet Gynecol* 2012; 39:203-209.

75.   Gómez O, Soveral I, Bennasar M, et al. Accuracy of fetal echocardiography in the differential diagnosis between truncus arteriosus and pulmonary atresia with ventricular septal defect. *Fetal Diagn Ther* 2016; 39:90-99.

76.   Yeo L, Romero R. Intelligent navigation to improve obstetrical sonography. *Ultrasound Obstet Gynecol* 2016; 47: 403-409.

77.   Yeo L, Romero R. Fetal Intelligent Navigation Echocardiography (FINE): a novel method for rapid, simple, and automatic examination of the fetal heart. *Ultrasound Obstet Gynecol* 2013; 42:268-284.

78.   Garcia M, Yeo L, Romero R, et al. Prospective evaluation of the fetal heart using Fetal Intelligent Navigation Echocardiography (FINE). *Ultrasound Obstet Gynecol* 2016; 47:450-459.

79. Veronese P, Bogana G, Cerutti A, Yeo L, Romero R, Gervasi MT. A prospective study of the use of fetal intelligent navigation echocardiography (FINE) to obtain standard fetal echocardiography views. *Fetal Diagn Ther* 2017; 41:89-99.

80. Yeo L, Luewan S, Markush D, Gill N, Romero R. Prenatal diagnosis of dextrocardia with complex congenital heart disease using fetal intelligent navigation echocardiography (FINE) and a literature review [published online ahead of print June 23, 2017]. *Fetal Diagn Ther*. doi: 10.1159/000468929.

81. Evans MI, Galen RS, Britt DW. Principles of screening. *Semin Perinatol* 2005; 29:364-366.

82. Allan LD, Sharland GK, Milburn A, et al. Prospective diagnosis of 1,006 consecutive cases of congenital heart disease in the fetus. *J Am Coll Cardiol* 1994; 23:1452-1458.

83. Angiulli A, Tai A, Easterbrook S. Voluson: Electronic 4D imaging – Designed for Women's Health. *GE Healthcare;* September 2014.

84. Guasina F, Bellussi F, Morganelli G, Salsi G, Pilu G, Simonazzi G. Electronic STIC improves four-dimensional fetal echocardiography [published online ahead of print March 24, 2017]. *Ultrasound Obstet Gynecol*. doi:10.1002/uog.17474.

85. Deeks JJ, Altman DG. Diagnostic tests 4: likelihood ratios. *BMJ* 2004; 329:168-169.

86. Jaeschke R, Guyatt G, Lijmer J. Diagnostic tests. In: Guyatt G, Rennie D (eds). *Users' Guides to the Medical Literature.* Chicago, IL: AMA Press; 2002:121-140.

87. Gonçalves LF, Espinoza J, Romero R, et al. Four-dimensional ultrasonography of the fetal heart using a novel Tomographic Ultrasound Imaging display. *J Perinat Med* 2006; 34:39-55.

88. Aguilera M, Dummer K. Concordance of fetal echocardiography in the diagnosis of congenital cardiac disease utilizing updated guidelines [published online ahead of print March 12, 2017]. *J Matern Fetal Neonatal Med.* doi: 10.1080/14767058.2017.1297791.

89. Galindo A, Mendoza A, Arbues J, Grañeras A, Escribano D, Nieto O. Conotruncal anomalies in fetal life: accuracy of diagnosis, associated defects and outcome. *Eur J Obstet Gynecol Reprod Biol* 2009; 146:55-60.

90. Paladini D, Rustico M, Todros T, et al. Conotruncal anomalies in prenatal life. *Ultrasound Obstet Gynecol* 1996; 8:241–246.

91. Tometzki AJP, Suda K, Khol T, Kovalchin JP, Silverman NH. Accuracy of prenatal echocardiographic diagnosis and prognosis of fetuses with conotruncal anomalies. *J Am Coll Cardiol* 1999; 33:1696–1701.

92. Sivanandam S, Glickstein JS, Printz BF, et al. Prenatal diagnosis of conotruncal malformations: diagnostic accuracy, outcome, chromosomal abnormalities and extracardiac anomalies. *Am J Perinatol* 2006; 23:241–245.

Table 1.   Features of Fetal Intelligent Navigation Echocardiography (FINE) method

Feature	Definition
Intelligent navigation technology	New method of interrogation of a volume dataset whereby identification and selection of key anatomical landmarks allows the system to: 1) generate a geometrical reconstruction of the organ of interest (e.g. fetal heart); and 2) automatically navigate, find, extract, and display specific diagnostic planes
STICLoop™	Two-dimensional cine loop tool developed to aid the user in determining the appropriateness of STIC volume datasets before applying the FINE method to such volumes STICLoop criteria: 1) Fetal spine located between the 5- and 7-o'clock positions (reducing the possibility of shadowing from the ribs or spine) 2) Minimal or absent shadowing (including the three vessels and trachea view) which could obscure visualization of cardiac anatomy 3) Adequate image quality 4) Upper mediastinum and stomach included within the volume and clearly visible 5) Minimal or no motion artifacts observed in the STICLoop (i.e. smooth sweep without evidence of abrupt jumps or discontinuous movements) 6) Chest circumference contained with the region of interest 7) Sequential axial planes parallel to each other, similar to a sliced loaf of bread (i.e. no 'drifting spine' from the four-chamber view down to the stomach) 8) No azimuthal issues observed (i.e. atria/ventricles do not appear foreshortened in the four-chamber view) 9) Minimal or no motion artifacts observed in the sagittal plane
Anatomic Box®	Tool used to mark seven anatomical structures of the fetal heart within the STIC volume to generate a geometrical model of the fetal heart: 1) Cross-section of the aorta at the level of the stomach 2) Cross-section of the aorta at the level of the four-chamber view 3) Crux 4) Right atrial wall 5) Pulmonary valve 6) Cross-section of the superior vena cava 7) Transverse aortic arch

37

Diagnostic planes	Nine standard fetal echocardiography views automatically displayed by FINE in a single template: 1) Four chamber 2) Five chamber 3) Left ventricular outflow tract 4) Short-axis view of great vessels/right ventricular outflow tract 5) Three vessels and trachea 6) Abdomen/stomach 7) Ductal arch 8) Aortic arch 9) Superior and inferior vena cava
Automatic labeling	• Fetal echocardiography views, anatomical structures (atrial and ventricular chambers, great vessels, venae cavae and stomach), left and right side of fetus, and cranial and caudal ends • Labeling stays with the corresponding anatomical structure(s), even as the image is increased or decreased in size
Virtual Intelligent Sonographer Assistance (VIS-Assistance®)	Operator-independent sonographic navigation and exploration of surrounding structures in a cardiac diagnostic plane of interest ('virtual' sonographer) • *Double VIS-Assistance*: technique in which VIS-Assistance is applied twice to a diagnostic plane of interest, allowing expanded navigational movements and further exploration • *Triple VIS-Assistance*: technique in which VIS-Assistance is applied three times to a diagnostic plane of interest, allowing expanded navigational movements and further exploration
Intelligent alerts	• Captions and/or a movie notifying the user about potential issues with the STIC volume dataset. The movies depict reference examples to guide and teach the operator. • If intelligent alerts appear, this will occur during the marking process • Three types: 1) *Breech alert*: notifies user that the fetus appears to be in a breech presentation; 2) *Possible drifting spine alert*: notifies user that there may be a 'drifting' fetal spine in the volume dataset (i.e. when the spine location migrates on the screen); and 3) *Spine location alert*: notifies user that the fetal spine appears to be located at a position different from what is recommended (i.e. between 5- and 7- o'clock). Once a spine location alert has appeared, three Marking alerts will appear next in sequence. o A spine location alert will only appear if the fetal spine is located at these "times" (o'clock): 12, 1, 2, 3, 4, between 4 and 5, between 7 and 8, 8, 9, 10, 11

38

| Marking alerts | • Captions/movies notifying the user that fetal anatomical structures for marking (e.g. pulmonary valve) may be in a different location than what is expected. The movies depict reference examples to guide and teach the operator.
 • Marking alerts occur during the marking process, and will only appear if the Spine location alert has already appeared
 • Three types: 1) *Pulmonary valve alert*; 2) *Superior vena cava alert*; and 3) *Transverse aortic arch alert* |

STIC, spatiotemporal image correlation

Table 2. Fetal Intelligent Navigation Echocardiography (FINE): success rates of obtaining nine fetal echocardiography views after applying intelligent navigation to 100 normal spatiotemporal image correlation (STIC) volume datasets using diagnostic planes and/or Virtual Intelligent Sonographer Assistance (VIS-Assistance)

Fetal echocardiography view	Diagnostic plane (n=100)		VIS-Assistance (n=100)		Diagnostic plane and/or VIS-Assistance (n=100)	
	n (%)	95% CI*	n (%)	95% CI*	n (%)	95% CI*
1. Four-chamber	97 (97)	91 to 99	100 (100)	96 to 100	100 (100)	96 to 100
2. Five-chamber	99 (99)	94 to > 99.9	100 (100)	96 to 100	100 (100)	96 to 100
3. LVOT	99 (99)	94 to > 99.9	100 (100)	96 to 100	100 (100)	96 to 100
4. Short axis view of great vessels/RVOT	97 (97)	91 to 99	100 (100)	96 to 100	100 (100)	96 to 100
5. 3VT	99 (99)	94 to > 99.9	100 (100)	96 to 100	100 (100)	96 to 100
6. Abdomen/Stomach	100 (100)†	96 to 100	100 (100)‡	96 to 100	100 (100)	96 to 100
7. Ductal arch	95 (95)	95 to 100	100 (100)	96 to 100	100 (100)	96 to 100
8. Aortic arch	98 (98)	95 to 100	100 (100)	96 to 100	100 (100)	96 to 100
9. SVC/IVC	94 (94)	95 to 100	100 (100)	96 to 100	100 (100)	96 to 100
• SVC	97 (97)	91 to 99	--	--	--	--
• IVC	97 (97)	91 to 99	--	--	--	--

*The Wald method was used to calculate two-sided CIs for proportions expressed in the table; as the true proportion cannot exceed 100%, upper confidence limits are truncated at 100%.
†Defined as visualization of the stomach in the diagnostic plane

40

‡Defined as visualization of both the stomach and four-chamber view in VIS-Assistance® (to determine situs)

3VT, three vessels and trachea; IVC, inferior vena cava; LVOT, left ventricular outflow tract; RVOT, right ventricular outflow tract; SVC, superior vena cava.

41

Table 3.   Main categories of congenital heart defects evaluated by the FINE method

Congenital heart defect	n (%)
Conotruncal anomalies	**21 (42)**
Tetralogy of Fallot*	9 (18)
DORV	5 (10)
Complete TGV	4 (8)
Pulmonary atresia with VSD	2 (4)
Truncus arteriosus	1 (2)
Left heart anomalies	**10 (20)**
Coarctation of aorta	5 (10)
Hypoplastic left heart	4 (8)
Interrupted aortic arch	1 (2)
Right heart anomalies	**8 (16)**
Pulmonary atresia with intact ventricular septum	3 (6)
Tricuspid atresia with VSD	2 (4)
Pulmonary stenosis	2 (4)
Ebstein anomaly	1 (2)
Complex cardiac defects	**6 (12)**
Small RV, VSD, small pulmonary artery, large pericardial effusion	1 (2)
Hypoplastic left heart, DORV, TGV, stomach on fetal right side	1 (2)
Double inlet left ventricle, TGV, pulmonary stenosis, ASD, left SVC	1 (2)
Double inlet right ventricle, DORV, coarctation of aorta	1 (2)
Interrupted IVC with azygos vein continuation; stomach on right side	1 (2)
LV non-compaction, dilated cardiomyopathy, left SVC, secundum ASD, VSD, hypoplastic tricuspid valve	1 (2)
Septal defects	**5 (10)**
Atrioventricular septal defect	3 (6)
VSD	2 (4)
TOTAL	**50**

*Includes the following types (n=3): 1) tetralogy of Fallot with right aortic arch; 2) tetralogy of Fallot with absent pulmonary valve; 3) tetralogy of Fallot with absent pulmonary valve, right aortic arch, vascular ring

ASD, atrial septal defect; DORV, double outlet right ventricle; IVC, inferior vena cava; LV, left ventricle; RV, right ventricle; SVC, superior vena cava; TGV, transposition of the great vessels; VSD, ventricular septal defect

42

Table 4. Characteristics of FINE fundamental in determining whether the fetal heart is abnormal or not, and in determining the specific cardiac diagnosis

Characteristic	FINE
General	• Automatic realignment of STIC volume, and reorientation and standardization of the anatomical position so that the fetus and cardiac diagnostic planes are consistently displayed in the same manner each time
No manual navigation	• Manual standardization or manipulation of the STIC volume dataset and reference planes is not required (e.g. alignment or rotation) • Reduced operator dependency • Examination of the fetal heart is standardized and simplified
STICLoop™	• While the two-dimensional cine loop is automatically scrolling in a continuous fashion, abnormal cardiac anatomy is often displayed
Marking of anatomical structures within the STIC volume	• During the marking process, sometimes it is evident that: 1) anatomical structures are absent; 2) anatomical structures are not in their usual location; or 3) marking anatomical structures is difficult. One explanation is the presence of CHD.
Cardiac diagnostic planes	• All nine planes (including transverse and sagittal) are displayed simultaneously in a single template • Various features of the CHD can be visualized and compared side-by-side (e.g. overriding aorta, ventricular septal defect, pulmonary stenosis in tetralogy of Fallot) • Same specific abnormality can be confirmed in multiple echocardiography views at the same time (e.g. hypoplasia of the pulmonary artery seen in the 3VT view, short-axis view of great vessels/right ventricular outflow tract, and ductal arch view)
VIS-Assistance®	• Depiction of cardiac abnormalities when the diagnostic plane appears normal • Provides further diagnostic information even when the diagnostic plane is abnormal • Changes a suspected abnormal fetal echocardiography view to one that is interpreted as normal • Improves the success of obtaining the fetal echocardiography view of interest when this is not initially obtained via the diagnostic plane • Double, triple VIS-Assistance techniques
Automatic labeling	• Assists in identification of fetal echocardiography views, anatomical structures (atrial and ventricular chambers, great vessels, venae cavae and stomach), left and right side of fetus, and cranial and caudal ends

43

Color Doppler FINE	Depicts abnormal fetal cardiac anatomy and/or hemodynamic flow characteristics

3VT, three vessels and trachea view; CHD, congenital heart defect; STIC, spatiotemporal image correlation; VIS-Assistance®, Virtual Intelligent Sonographer Assistance

Table 5. Details of congenital heart defect cases with major discordancy between the FINE diagnosis compared to final diagnosis

GA (weeks)	FINE Diagnosis	Final Diagnosis
19	Complete atrioventricular septal defect, univentricle, large VSD, pulmonary stenosis, DORV, TGV, stomach on fetal right side	Hypoplastic left heart, DORV, TGV, stomach on fetal right side
21	Tetralogy of Fallot	Pulmonary atresia, VSD
22	Left ventricle smaller than right ventricle, dilated left atrium, mitral dysplasia, aortic stenosis, VSD, DORV, left SVC, small pulmonary artery	Variant of hypoplastic left heart, mitral dysplasia, aortic atresia, VSD
26	Normal	Pulmonary artery branch stenosis, small secundum ASD
30	Tetralogy of Fallot	Pulmonary atresia, VSD, supravalvular aortic stenosis
35	LV non-compaction, dilated cardiomyopathy, left SVC, VSD, aortic stenosis, small pulmonary artery and ductus arteriosus, hypoplastic and dysplastic tricuspid valve	LV non-compaction, dilated cardiomyopathy, left SVC, VSD, secundum ASD, hypoplastic tricuspid valve
37	Tetralogy of Fallot	DORV, VSD, pulmonary stenosis, left SVC

ASD, atrial septal defect; DORV, double outlet right ventricle; GA, gestational age; LV, left ventricle; SVC, superior vena cava; TGV, transposition of great vessels; VSD, ventricular septal defect

45

Video Legends

Video 1: Nine normal cardiac diagnostic planes in a single template with the unique feature of automatic labeling (through intelligent navigation) of each plane, anatomical structures, fetal left and right sides, and cranial and caudal ends (also see Figure 1). The labeling is distinctive because it stays with the corresponding anatomical structure(s), even as the image is increased or decreased in size. *A, transverse aortic arch; Ao, aorta; Desc., descending; IVC, inferior vena cava; LA, left atrium; LV, left ventricle; P, pulmonary artery; PA, pulmonary artery; RA, right atrium; RV, right ventricle; RVOT, right ventricular outflow tract; S, superior vena cava; SVC, superior vena cava; Trans., transverse*

Video 2: Application of the FINE method to a fetus with tetralogy of Fallot at 23 weeks of gestation (diagnostic planes or VIS-Assistance with automatic labeling are shown) (also see Figure 2). Six echocardiography views were abnormal and demonstrate the typical features of this cardiac defect. The three vessels and trachea view shows a narrow pulmonary artery due to stenosis, while the transverse aortic arch is prominent. There is a 'Y-shaped' appearance of the great vessels. As is commonly noted in conotruncal abnormalities, the four-chamber view appeared normal in the diagnostic plane; however, VIS-Assistance demonstrates a large ventricular septal defect (not shown here). The five-chamber view shows a ventricular septal defect. The left ventricular outflow tract view shows an overriding aorta, dilated aortic root, and ventricular septal defect. In the short axis view of great vessels/right ventricular outflow tract (obtained via VIS-Assistance), the pulmonary artery is narrow with a tortuous ductus arteriosus. There is difficulty in visualizing a normal ductal arch. In the aortic arch view, the aortic root is dilated and there is a prominent ascending aorta. *A, transverse aortic arch; Ao, aorta; Desc., descending; IVC, inferior vena cava; LA, left atrium; LV, left ventricle; P, pulmonary artery; PA, pulmonary artery; RA, right atrium; RV, right ventricle; RVOT, right ventricular outflow tract; S, superior vena cava; SVC, superior vena cava; Trans., transverse*

Video 3: Application of the FINE method to a fetus with coarctation of the aorta at 24 weeks of gestation (diagnostic planes or VIS-Assistance with automatic labeling are shown) (also see Figure 3). Seven echocardiography views are abnormal. The three vessels and trachea view shows a narrow transverse aortic arch. In the four-chamber view, the left side of the heart is smaller than the right side; however, the left ventricle is apex-forming and there is good movement of the mitral valve. The right side of the heart appears enlarged, with the right ventricle being moderately dilated and hypertrophied. The five-chamber view shows similar findings to that of the four-chamber view. In addition, there is a narrow aortic root. The left ventricular outflow tract view shows a narrow aorta (obtained via VIS-Assistance). In the short-axis view of great vessels/right ventricular outflow tract, the cross-section of the aorta is small compared to the pulmonary artery. The enlarged right atrium is apparent. The ductal arch view demonstrates that the cross-section of the aorta is small compared to the pulmonary artery. In the aortic arch view, the coarctation is demonstrated as hypoplasia and narrowing of the transverse aortic arch as well as in the isthmus region. *A, transverse aortic arch; Ao, aorta; Desc., descending; IVC, inferior vena cava; LA, left atrium; LV, left ventricle; P, pulmonary artery; PA, pulmonary artery; RA, right atrium; RV, right ventricle; RVOT, right ventricular outflow tract; S, superior vena cava; SVC, superior vena cava; Trans., transverse*

46

<u>Video 4</u>: VIS-Assistance of the left ventricular outflow tract view in a 19 week fetus with hypoplastic left heart, double outlet right ventricle, transposition of the great vessels, and fetal stomach on the right side (also see Figure 4). The abnormal diagnostic plane (left panel) demonstrates a single vessel arising from the right ventricle that is consistent with the pulmonary artery due to its bifurcation. A second vessel could not be clearly identified. However, when VIS-Assistance is activated (right panel), automatic navigational movements now demonstrate a second vessel (aorta) which is rightward and anterior, and exiting the right ventricle. These two vessels (indicated by white arrows) are parallel and side-by-side, consistent with transposition.

47

Figure Legends

Figure 1: Application of the Fetal Intelligent Navigation Echocardiography (FINE) method to a fetus with a normal fetal heart. Nine normal cardiac diagnostic planes in a single template are shown with the unique feature of automatic labeling (through intelligent navigation) of each plane, anatomical structures, fetal left and right sides, and cranial and caudal ends (also see Video 1). The labeling is distinctive because it stays with the corresponding anatomical structure(s), even as the image is increased or decreased in size. *A, transverse aortic arch; Ao, aorta; Desc., descending; IVC, inferior vena cava; LA, left atrium; LV, left ventricle; P, pulmonary artery; PA, pulmonary artery; RA, right atrium; RV, right ventricle; RVOT, right ventricular outflow tract; S, superior vena cava; SVC, superior vena cava; Trans., transverse*

Figure 2: Application of the FINE method to a fetus with tetralogy of Fallot at 23 weeks of gestation (diagnostic planes or VIS-Assistance with automatic labeling are shown) (also see Video 2). Six echocardiography views were abnormal and demonstrate the typical features of this cardiac defect. The three vessels and trachea view shows a narrow pulmonary artery due to stenosis, while the transverse aortic arch is prominent. There is a 'Y-shaped' appearance of the great vessels. As is commonly noted in conotruncal abnormalities, the four-chamber view appeared normal in the diagnostic plane; however, VIS-Assistance demonstrates a large ventricular septal defect (not shown here). The five-chamber view shows a ventricular septal defect. The left ventricular outflow tract view shows an overriding aorta, dilated aortic root, and ventricular septal defect. In the short axis view of great vessels/right ventricular outflow tract (obtained via VIS-Assistance), the pulmonary artery is narrow with a tortuous ductus arteriosus. There is difficulty in visualizing a normal ductal arch. In the aortic arch view, the aortic root is dilated and there is a prominent ascending aorta. *A, transverse aortic arch; Ao, aorta; Desc., descending; IVC, inferior vena cava; LA, left atrium; LV, left ventricle; P, pulmonary artery; PA, pulmonary artery; RA, right atrium; RV, right ventricle; RVOT, right ventricular outflow tract; S, superior vena cava; SVC, superior vena cava; Trans., transverse*

Figure 3: Application of the FINE method to a fetus with coarctation of the aorta at 24 weeks of gestation (diagnostic planes or VIS-Assistance with automatic labeling are shown) (also see Video 3). Seven echocardiography views are abnormal. The three vessels and trachea view shows a narrow transverse aortic arch. In the four-chamber view, the left side of the heart is smaller than the right side; however, the left ventricle is apex-forming. The right side of the heart appears enlarged, with the right ventricle being moderately dilated and hypertrophied. The five-chamber view shows similar findings to that of the four-chamber view. In addition, there is a narrow aortic root. The left ventricular outflow tract view shows a narrow aorta (obtained via VIS-Assistance). In the short-axis view of great vessels/right ventricular outflow tract, the cross-section of the aorta is small compared to the pulmonary artery. The enlarged right atrium is apparent. The ductal arch view demonstrates that the cross-section of the aorta is small compared to the pulmonary artery. In the aortic arch view, the coarctation is demonstrated as hypoplasia and narrowing of the transverse aortic arch as well as in the isthmus region. *A, transverse aortic arch; Ao, aorta; Desc., descending; IVC, inferior vena cava; LA, left atrium; LV, left ventricle; P, pulmonary artery; PA, pulmonary artery; RA, right atrium; RV, right ventricle; RVOT, right ventricular outflow tract; S, superior vena cava; SVC, superior vena cava; Trans., transverse*

48

Figure 4: VIS-Assistance of the left ventricular outflow tract view in a 19 week fetus with hypoplastic left heart, double outlet right ventricle, transposition of the great vessels, and fetal stomach on the right side (also see Video 4). The abnormal diagnostic plane (left panel) demonstrates a single vessel arising from the right ventricle that is consistent with the pulmonary artery due to its bifurcation. A second vessel could not be clearly identified. However, when VIS-Assistance is activated (right panel), automatic navigational movements now demonstrate a second vessel (aorta) which is rightward and anterior, and exiting the right ventricle. These two vessels are parallel and side-by-side, consistent with transposition. *AO, aorta; PA, pulmonary artery; RV, right ventricle.*
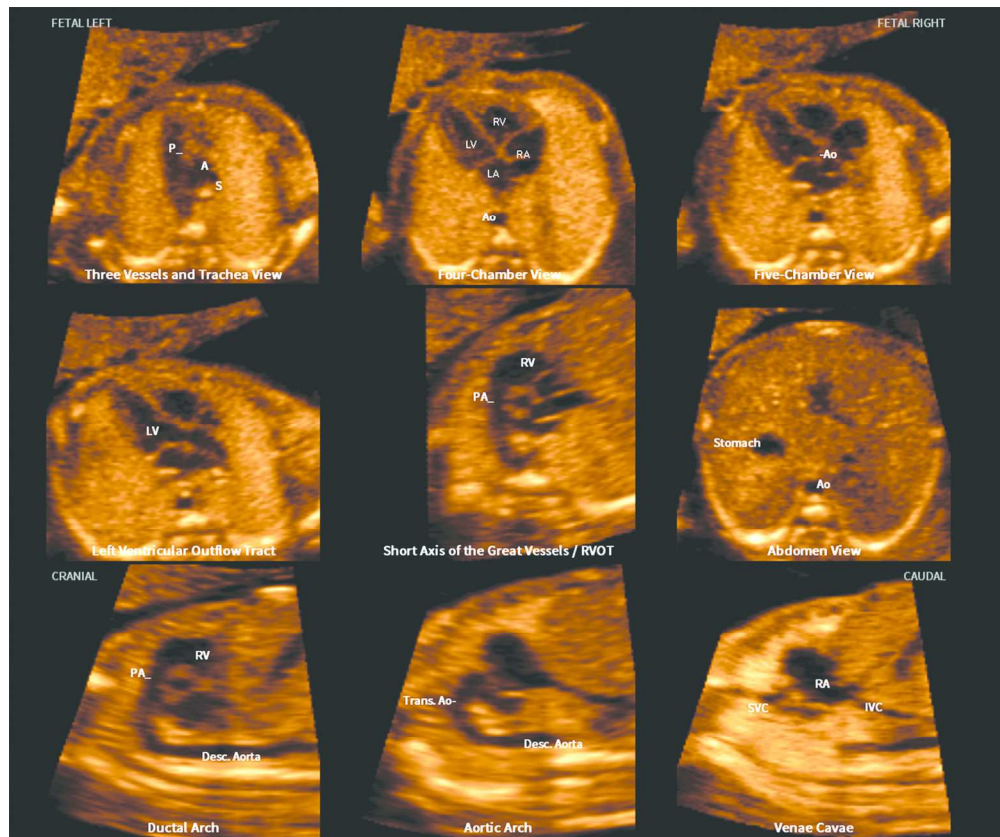
Figure 1: Application of the Fetal Intelligent Navigation Echocardiography (FINE) method to a fetus with a normal fetal heart. Nine normal cardiac diagnostic planes in a single template are shown with the unique feature of automatic labeling (through intelligent navigation) of each plane, anatomical structures, fetal left and right sides, and cranial and caudal ends (also see Video 1). The labeling is distinctive because it stays with the corresponding anatomical structure(s), even as the image is increased or decreased in size. A, transverse aortic arch; Ao, aorta; Desc., descending; IVC, inferior vena cava; LA, left atrium; LV, left ventricle; P, pulmonary artery; PA, pulmonary artery; RA, right atrium; RV, right ventricle; RVOT, right ventricular outflow tract; S, superior vena cava; SVC, superior vena cava; Trans., transverse
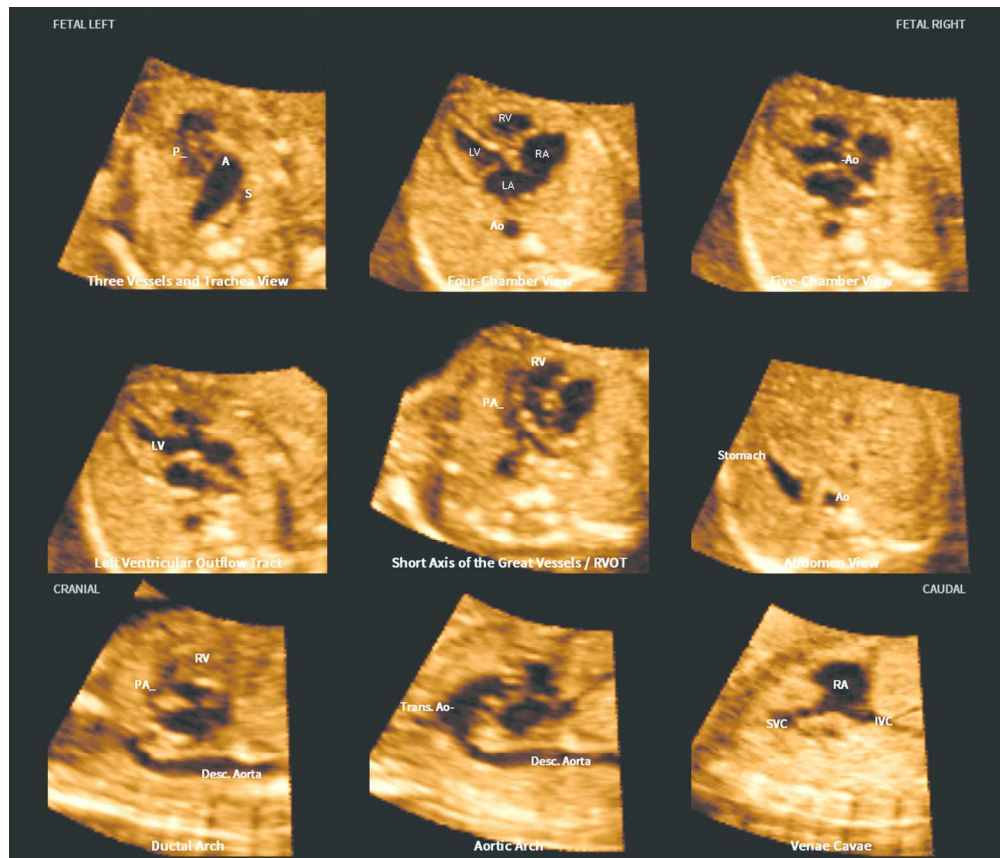
137x114mm (300 x 300 DPI)

Figure 2: Application of the FINE method to a fetus with tetralogy of Fallot at 23 weeks of gestation (diagnostic planes or VIS-Assistance with automatic labeling are shown) (also see Video 2). Six echocardiography views were abnormal and demonstrate the typical features of this cardiac defect. The three vessels and trachea view shows a narrow pulmonary artery due to stenosis, while the transverse aortic arch is prominent. There is a 'Y-shaped' appearance of the great vessels. As is commonly noted in conotruncal abnormalities, the four-chamber view appeared normal in the diagnostic plane; however, VIS-Assistance demonstrates a large ventricular septal defect (not shown here). The five-chamber view shows a ventricular septal defect. The left ventricular outflow tract view shows an overriding aorta, dilated aortic root, and ventricular septal defect. In the short axis view of great vessels/right ventricular outflow tract (obtained via VIS-Assistance), the pulmonary artery is narrow with a tortuous ductus arteriosus. There is difficulty in visualizing a normal ductal arch. In the aortic arch view, the aortic root is dilated and there is a prominent ascending aorta. A, transverse aortic arch; Ao, aorta; Desc., descending; IVC, inferior vena cava; LA, left atrium; LV, left ventricle; P, pulmonary artery; PA, pulmonary artery; RA, right atrium; RV, right ventricle; RVOT, right ventricular outflow tract; S, superior vena cava; SVC, superior vena cava; Trans., transverse
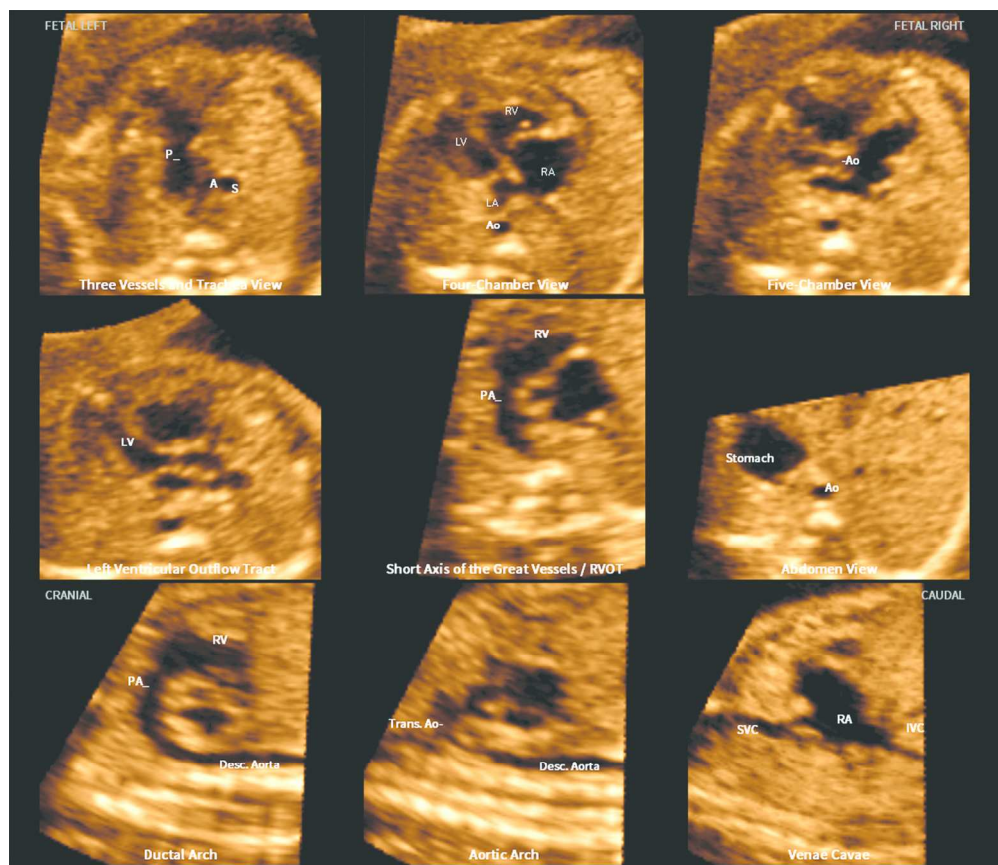
140x119mm (300 x 300 DPI)

Figure 3: Application of the FINE method to a fetus with coarctation of the aorta at 24 weeks of gestation (diagnostic planes or VIS-Assistance with automatic labeling are shown) (also see Video 3). Seven echocardiography views are abnormal. The three vessels and trachea view shows a narrow transverse aortic arch. In the four-chamber view, the left side of the heart is smaller than the right side; however, the left ventricle is apex-forming. The right side of the heart appears enlarged, with the right ventricle being moderately dilated and hypertrophied. The five-chamber view shows similar findings to that of the four-chamber view. In addition, there is a narrow aortic root. The left ventricular outflow tract view shows a narrow aorta (obtained via VIS-Assistance). In the short-axis view of great vessels/right ventricular outflow tract, the cross-section of the aorta is small compared to the pulmonary artery. The enlarged right atrium is apparent. The ductal arch view demonstrates that the cross-section of the aorta is small compared to the pulmonary artery. In the aortic arch view, the coarctation is demonstrated as hypoplasia and narrowing of the transverse aortic arch as well as in the isthmus region. A, transverse aortic arch; Ao, aorta; Desc., descending; IVC, inferior vena cava; LA, left atrium; LV, left ventricle; P, pulmonary artery; PA, pulmonary artery; RA, right atrium; RV, right ventricle; RVOT, right ventricular outflow tract; S, superior vena cava; SVC, superior vena cava; Trans., transverse
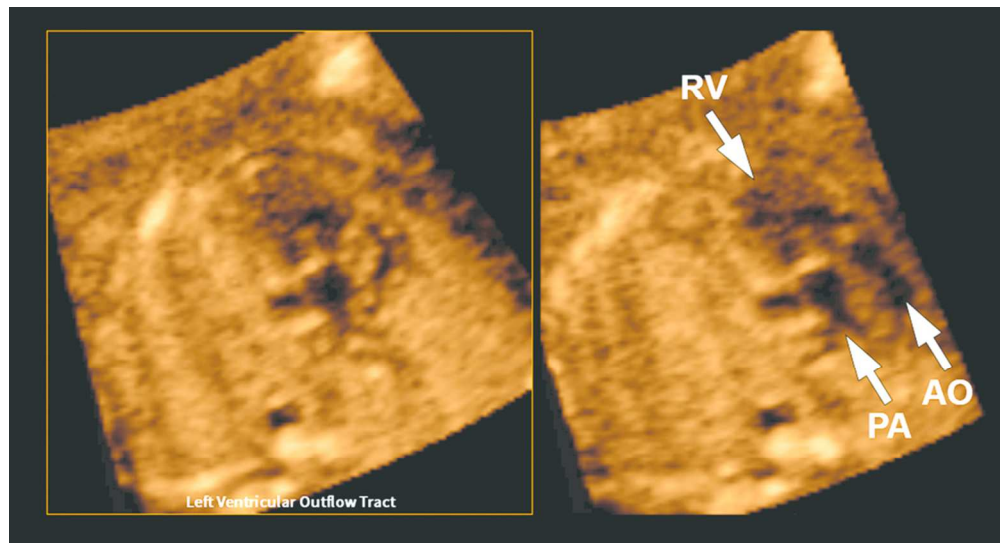
141x121mm (300 x 300 DPI)

Figure 4: VIS-Assistance of the left ventricular outflow tract view in a 19 week fetus with hypoplastic left heart, double outlet right ventricle, transposition of the great vessels, and fetal stomach on the right side (also see Video 4). The abnormal diagnostic plane (left panel) demonstrates a single vessel arising from the right ventricle that is consistent with the pulmonary artery due to its bifurcation. A second vessel could not be clearly identified. However, when VIS-Assistance is activated (right panel), automatic navigational movements now demonstrate a second vessel (aorta) which is rightward and anterior, and exiting the right ventricle. These two vessels are parallel and side-by-side, consistent with transposition. AO, aorta; PA, pulmonary artery; RV, right ventricle.

89x48mm (300 x 300 DPI)